Computational Characterization of a Composite Ceramic Block for a Millimeter Wave Heat Exchanger

Petra Kumi, Jonathan S. Venne, Vadim V. Yakovlev, Martin S. Hilario, Brad W. Hoff, and Ian M. Rittersdorf

Abstract Electromagnetic and electromagnetic-thermal coupled problems are solved by the finite-difference time-domain technique for an AlN:Mo composite ceramic block backed by a thin metal plate and irradiated by a high-power W-band plane wave. Computation is based on experimental data on temperature-dependent complex permittivity, specific heat, and thermal conductivity. Non-uniformity of patterns of dissipated power and temperature is quantified via standard-deviation-based metrics. A $10\times10\times10\pm2$ mm block of the composite with concentration of Mo from 0.25 to 4% is considered as irradiated by the plane wave with power density on the block's front surface from 0.3 to 1.0 W/mm^2 at 95 GHz. It is shown that the block can be heated up to 1000 ^{o}C highly uniformly for 50–110 s. The composite producing maximum total dissipated power is found to have Mo content about 3%.

1 Introduction

Electromagnetic (EM) heating is employed in applications in food engineering, chemistry, materials science [1, 2]. This phenomenon is also in the core of recently introduced EM heat exchangers (HX) used in solar energy collectors [3], power beaming applications [4], and microwave thermal thrusters [5]. Millimeter-wave (MMW) powered HX are currently under development for the use in power beaming experiments for wireless energy transfer [6–8]. Interactions of the MMW field

P. Kumi · J. S. Venne · V. V. Yakovlev (✉)
Worcester Polytechnic Institute, Worcester, MA, USA
e-mail: pkumi@wpi.edu; jsvenne@wpi.edu; vadim@wpi.edu

M. S. Hilario · B. W. Hoff
Air Force Research Laboratory, Kirtland AFB, Albuquerque, NM, USA
e-mail: martin.hilario@us.af.mil; brad.hoff@us.af.mil

I. M. Rittersdorf
Naval Research Laboratory, Washington, DC, USA
e-mail: ian.rittersdorf@nrl.navy.mil

G. Nicosia, V. Romano (eds.), *Scientific Computing in Electrical Engineering*, Mathematics in Industry 32, https://doi.org/10.1007/978-3-030-44101-2_7

with ceramic slabs should be well understood for effectively utilizing EM energy, controllably heating the material, and transferring heat to fluid flowing through the neighboring channels.

In this paper, by the means of EM and coupled EM-thermal modeling, we study the process of heating of a rectangular block of an aluminum nitride-molybdenum (AlN:Mo) composite by a normally incident plane MMW. The back surface of the block is in contact with a thin metal plate. Characterizing this system in terms of homogeneity of heating and a level of absorbed power, we identify the material which appears to be most efficient for using in a physical prototype of a MMW HX.

2 Computational Scenario & Input Data

A considered MMW-powered HX contains an assembly of ceramic tiles and a metal baseplate that is attached to their back surfaces and contains channels with fluid flow (Fig. 1). Due to dielectric losses, EM power is dissipated inside the ceramic blocks and induces thermal field that heats the baseplate and the flowing fluid.

In order to help design the physical prototype, we build a computer model capable of simulating EM and thermal processes in a single ceramic block irradiated by a plane wave and attached to a thin metal plate (Fig. 2). An ultimate goal of the computational experiments is to find a composition of the AlN:Mo composite that leads to maximum absorption of EM energy and, at the same time, to as uniform temperature distribution on the back surface of the block as possible.

The considered factors affecting the system performance are limited to its EM and thermal material parameters: dielectric constant ϵ', the loss factor ϵ'', density ρ, specific heat c, and thermal conductivity k. We examine AlN samples with different levels of Mo doping; by varying percentage of Mo in the AlN:Mo composite, both EM and thermal parameters can be significantly changed.

Temperature characteristics of ϵ' and ϵ'' were obtained with the use of a dedicated apparatus for a free space dielectric measurement [7, 9] at 95 GHz for temperatures T up to nearly 550 ^{o}C. The measurements were carried out for six samples of AlN with Mo content from 0.25 to 4% by volume. The characteristics turned out to be almost linearly dependent on T (Fig. 3). Corresponding linear polynomials (also shown in Fig. 3) approximating the experimental data points were used to generate the values of ϵ' and ϵ'' at 20, 100, 200, ..., 1000 ^{o}C as input data for the EM model.

Fig. 1 Conceptual drawing of a section of a MMW-powered HX

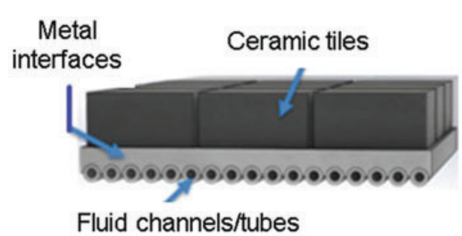

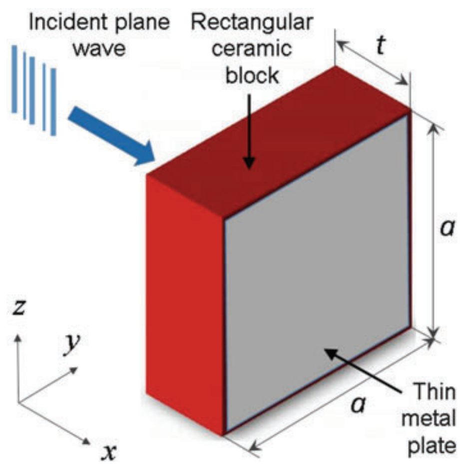

Fig. 2 3D view of the considered computational scenario

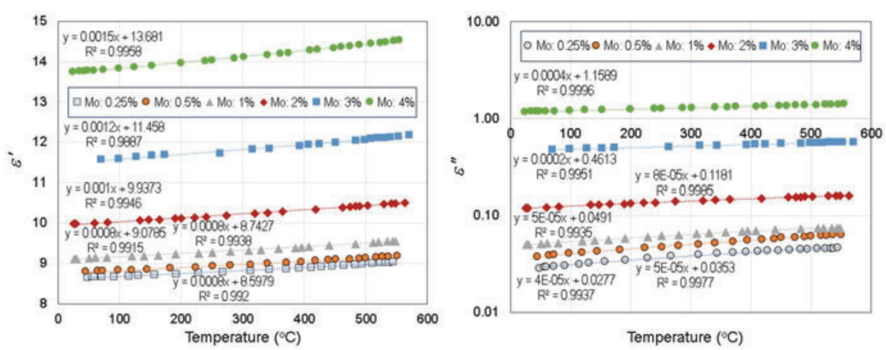

Fig. 3 Measured points and linearly approximated temperature characteristics of dielectric constant ϵ' and the loss factor ϵ'' of six AlN:Mo samples with different concentrations of Mo

Values of specific heat and thermal conductivity were measured for 4% of Mo at seven temperatures between 20 and 1001 ^{o}C (large points in Fig. 4), and they were assumed to be similar to those of lower concentrations of Mo. The values of c and k at the intermediate points (i.e., at 50, 150, 200, ..., 950 ^{o}C) were determined from cubic spline interpolations of the experimental points; those values are also shown in Fig. 4 (small points).

Density ρ was measured for 4% of Mo at room temperature and found to be 3.66 g/cm^3. It was used in all computations under the assumption that it does not depend on concentration of Mo and temperature.

Computations were carried out for the AlN:Mo block with a = 10 mm and t = 8, 10 and 12 mm. Thickness of the thin metal plate was 1 mm. The frequency of the incoming field was 95 GHz. The incident power of the plane wave was set as power density at the front surface of the composite block P_{in} being from 0.3 to 1.0 W/mm^2;

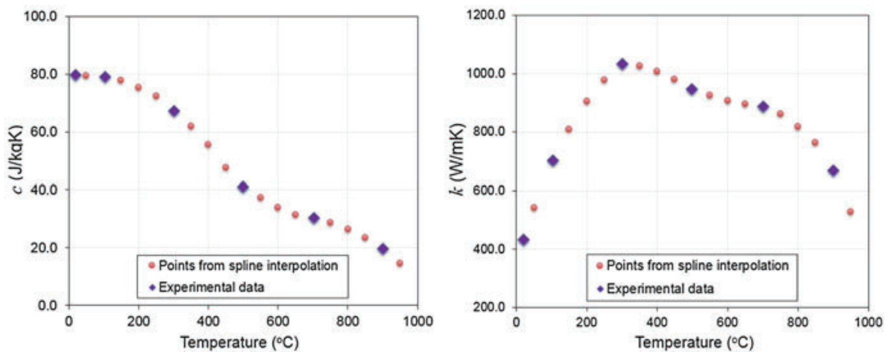

Fig. 4 Measured and spline-interpolated points of temperature characteristics of specific heat *c* and thermal conductivity *k* of the AlN:Mo sample with 4% concentrations of Mo

these values were expected to be consistent with the power and radiating antennas typical for MMW HX operations.

3 Computational Techniques

3.1 Electromagnetic and Thermal Problems

The process of MMW heating of an AlN:Mo block is studied with EM and EM-thermal (coupled) models. Both underlying (EM and thermal) problems are numerically solved by a 3D finite-difference time-domain (FDTD) technique. That is, similarly to the fundamental FDTD step with Maxwell's equations, both spatial and temporal partial derivatives in the heat transfer equation are approximated by the central-difference formula, and the differential equation is converted into an algebraic one. Both EM and thermal problems are discretized using the same mesh.

In order to satisfy the Courant condition and minimize computational resources, the scenario is discretized by the mesh with maximum cell sizes of 0.295 and 0.095 mm in air and in the material, respectively. The $t \times a \times a$ mm AlN:Mo block is surrounded by the $(t{+}8)\times(a{+}3)\times(a{+}3)$ mm plane wave box with one $(a{+}3)\times(a{+}3)$ mm face responsible for sinusoidal excitation of the incident field. The ceramic block is situated inside the $(t{+}14)\times(a{+}9)\times(a{+}9)$ mm box imitating the Mur with superabsorption boundary condition.

Depending on the size of the block, the model consists of 2.9 to 3.5 mil cells. It is capable of computing patterns of dissipated power density (P_d) in the volume of the composite due to dielectric losses. These patterns are identical to temperature distributions at the initial moment of heat dissipation due to thermal conductivity.

The heat transfer problem is solved under Neumann (adiabatic) boundary conditions on all ceramic-air and ceramic-metal interfaces.

The EM and thermal solvers operate as part of an iterative procedure in which a steady state solution of the EM problem becomes an input for the thermal problem, and, in the repeated runs of the EM solver, material parameters are upgraded in every cell in accordance with the temperature field outputted from the thermal solver. The latter determines temperature distribution induced after each heating time step τ; N steps are needed to reach maximum temperature of the process (1000 °C).

The above computational scheme mimics time evolution of the MMW-induced temperature field under the given temperature-dependent EM and thermal material parameters. The procedure employed for coupling the two solvers is similar to the ones outlined in [10, 11]. The models were built in the environment of the FDTD solver *QuickWave* that includes its thermal units *QW-BHM* and *QW-HFM* [12].

3.2 Metric of Uniformity and Total Dissipated Power

Sufficient homogeneity of heating of the ceramic block is one of the required features of a MMW HX. A formal metric of field (non-) uniformity is necessary for quantitative characterization of the patterns and formulation of corresponding optimization problems. Following discussions in [13], it is introduced for P_d fields as:

$$\lambda_P = \frac{\sigma}{\mu}, \tag{1}$$

where σ is the standard deviation of the P_d values in all FDTD cells in the block from the mean value μ. When dealing with temperature field evolving in time, metric (1) is applied to all n patterns (corresponding to n different temperatures, $n \leq N$, where N is number of heating time steps τ) representing the heating process. The latter is therefore characterized by the metric

$$\lambda_T = \frac{1}{n}\sum_{i=1}^{n}\frac{\sigma_i}{\mu_i}, \tag{2}$$

where σ_i is the standard deviation of the T values in all FDTD cells in the block from the mean value in the ith pattern μ_i. Evaluation of uniformity of 2D patterns is based on the values of P_d or T in a particular layer of FDTD cells, and for 3D patterns, $\lambda_{P,T}$ are found from the values in the cells in the block's volume.

Denoting the total power dissipated in the ceramic material as $\bar{P}_d$ and the power brought by the incident wave as P, we introduce parameter η as a measure of energy efficiency of the MMW heating process as

$$\eta = \frac{\bar{P}_d}{P}. \tag{3}$$

Since ϵ' and ϵ'' vary with temperature, the value of $\bar{P}_d$ is different for every T. To characterize the heating process in terms of total dissipated power, we calculate

$$\hat{P}_d = \frac{1}{n}\sum_{i=1}^{n} \bar{P}_{di},\ n \leq N, \tag{4}$$

where $\bar{P}_{di}$ is the total dissipated power after the ith heating time step, and find η in (3) by using $\hat{P}_d$ instead of $\bar{P}_d$.

4 Results and Discussion

Typical distributions of P_d obtained from the EM model are shown in Fig. 5. For T = 400 and 800 °C, the patterns were computed under the assumption that the material was heated uniformly and therefore the values of complex permittivity were the same throughout the block. Of particular interest is distribution of heat on the back surface, so patterns in Fig. 5 show distributions of dissipated power density in the last layer of the FDTD cells in the ceramic block that is perpendicular to the x-axis.

It appears that P_d patterns, regardless the level of doping, are characterized by vast amount of maxima/minima. When the metal plate is attached, the patterns essentially change. A number of "hot spots" spread over the area of 10×10 mm

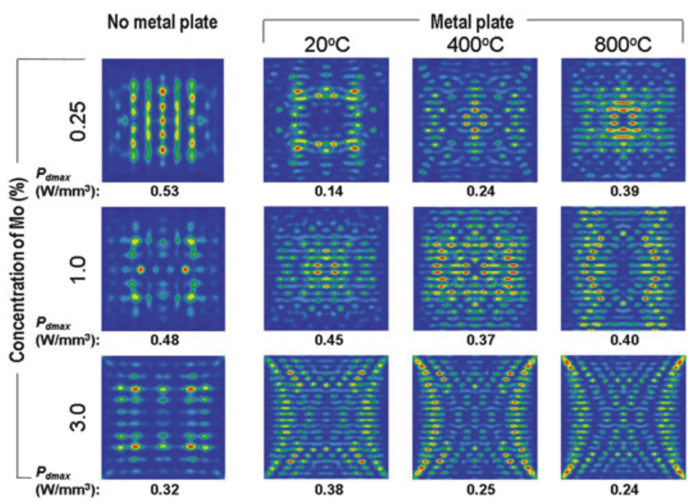

Fig. 5 Patterns of dissipated power density in the yz-plane on the back surface of the AlN:Mo block with 0.25, 1, and 3% of Mo at T = 20, 400, and 800 °C and maximum values of dissipated power density (P_{dmax}); P_{in} = 1 W/mm^2; t = 10 mm

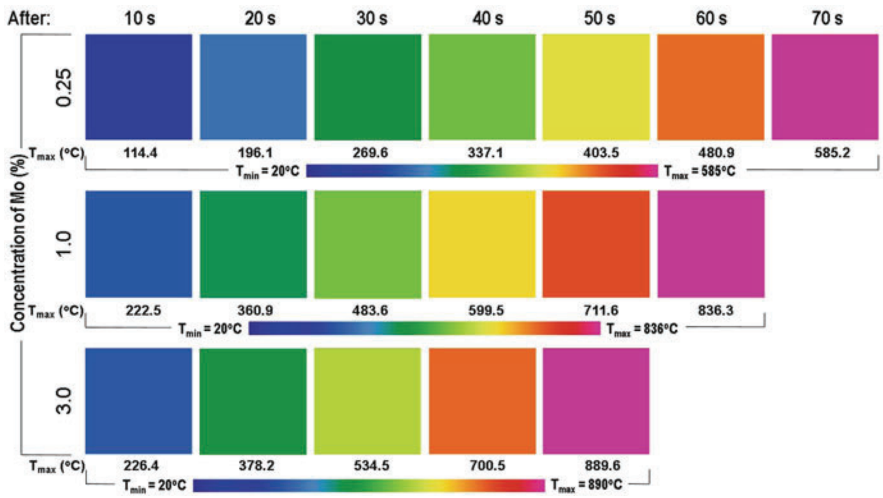

Fig. 6 Normalized temperature distributions in the yz-plane on the back surface of the AiN:Mo block with 0.25, 1, and 3% of Mo and maximum values of temperature (T_{max}); heating time steps 5 s (0.25% Mo), 2.5 s (1.0% Mo), 2 s (3.0% Mo); P_{in} = 1 W/mm^2; t = 10 mm

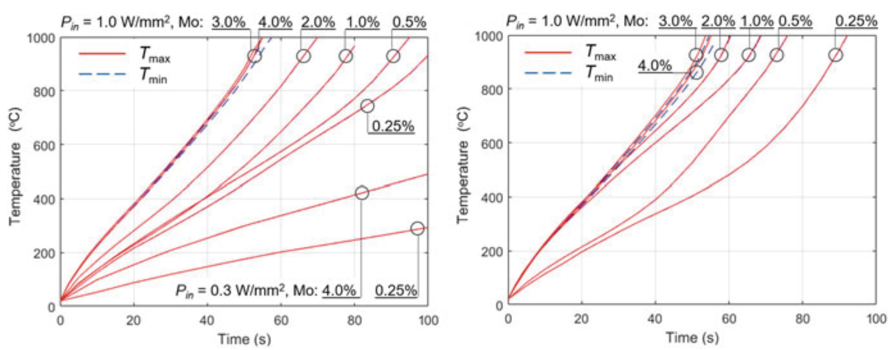

Fig. 7 Time evolution of maximum and minimum temperatures (T_{max} and T_{min}) of the MMW-heated AlN:Mo blocks with different concentrations of Mo (0.25 to 4%) and power densities of the incident wave P_{in} (0.3 and 1 W/mm^2); a thin metal plate is absent (left) and present (right); t = 10 mm

suggests that, due to high value of thermal conductivity of the AlN:Mo composites, the material may be heated sufficiently uniformly.

Temperature distributions obtained from the coupled model and shown in Fig. 6 depict the heating processes of three AlN:Mo blocks. Exceeding the expectation suggested by Fig. 5, the patterns are exceptionally uniform for all compositions of the material. (This, in turn, justifies the assumption about uniformity of heating that was used in computations of dissipated power in the EM model.)

The very high level of uniformity of temperature patterns in Fig. 6 (with λ_T in (2) being of the order of 10^{-4}) is also illustrated by the graphs in Fig. 7. It is seen that

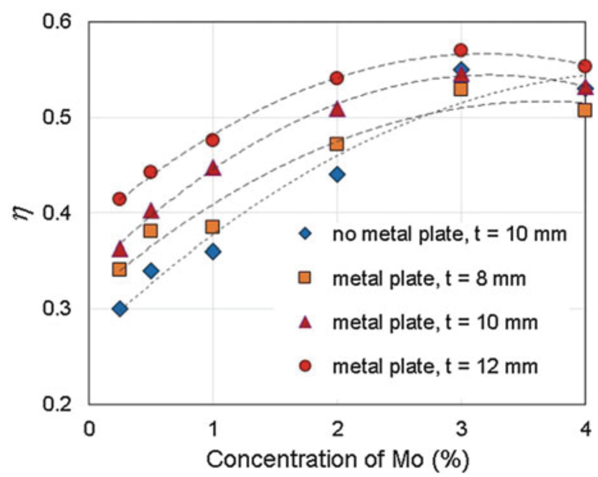

Fig. 8 Energy efficiency of the system with the thin metal plate absent and present

the time increases of minimum and maximum temperatures are almost identical; one can see small (5 to 50 ^{o}C) differences between T_{max} and T_{min} only in the composites with higher concentrations of Mo that are heated most rapidly.

When the power density of the incident field is 1 W/mm^2, temperature in the considered block reaches 1000 ^{o}C for the time between 50 and 110 s; the higher concentration of Mo, the faster the heating. This is due to the impact of composite's dielectric losses which notably increase with the rise of the contents of Mo.

When a back surface of the block is in contact with a metal plate, the composites with lower concentrations of Mo reach 1000 ^{o}C faster. The pace of heating for P_{in} = 1 W/mm^2 is found to be about three times higher than for 0.30 W/mm^2.

Parameter η in (3) computed for six Mo concentrations and the cases of absent and present metal plate reveals a maximum energy efficiency of the composites with Mo near 3% (Fig. 8). Variation in thickness (from 8 to 12 mm) does not affect the position of the maximum. The existence of the extreme value may be caused by a significant decay of both the incident and reflected fields in the blocks with high contents of Mo (3% and higher). The model may be built into a suitable optimization procedure searching for maximum energy efficiency of the system.

5 Conclusions

The performed computational studies allow for the following observations. When the plane wave carries the power of a practical level and that power is represented by the power density on the front surface of the composite block (so that P_{in} is from 0.3 to 1.0 W/mm^2), the AlN:Mo 10×10×10±2 mm samples are heated up to

1000 ^{o}C for 50–110 s, depending on the incoming power and concentration of Mo, and with a very high level of uniformity ($\lambda_T \approx 10^{-4}$). When the back surface of the ceramic block is in contact with a metal plate, absorption of MMW power is higher than in its absence.

While the blocks made of all the considered composites are heated highly uniformly, the materials with 3% concentration of molybdenum appear to be more energy efficient: for all thicknesses of the block, the parameter η takes on the largest values. On the other hand, preliminary data in production of the AlN:Mo composites suggests that the materials with Mo $\geq$ 3% are mechanically more stable and robust. The composites of those concentrations of Mo appear to be good candidates for the use in the physical prototype of a MMW-powered heat exchanger.

The developed EM-thermal coupled model is open for further development, and it is expected to be stimulated by the upcoming experimental studies. That may include the oblique incidence of the plane wave, multiple composite blocks on the metal plate, Gaussian beams, and alternative thermal boundary conditions imitating some particular operational regimes.

Acknowledgments J.S. Venne and V.V, Yakovlev are grateful for the support from the Air Force Research Laboratory (via Leidos, Inc.), Grant No P010200226. The work of P. Kumi was supported by the 2018 WPI Summer Undergraduate Research Fellowship (SURF). B.W. Hoff and M.S. Hilario were funded by the Air Force Office of Scientific Research under Contract FA9550-17RDCOR449 and by the Operational Energy Capability Improvement Fund (OECIF). I.M. Rittersdorf was supported by OECIF.

References

1. Willert-Porada, M.: Advances in Microwave and Radio Frequency Processing. Springer, Berlin (2006)
2. Leadbeater, N.: Microwave Heating as a Tool for Sustainable Chemistry. CRC Press, Boca Raton (2010)
3. Jamar, A., Majid, Z.A.A., Azmi, W.H., Norhafana, M., Razak, A.A.: A review of water heating system for solar energy applications. Int. Commun. Heat Mass Transfer **76**, 178–187 (2016)
4. Jawdat, B., Hoff, B., Hilario, M., Baros, A., Pelletier, P., Sabo, T., Dynys, F.: Composite ceramics for power beaming. In: Proc. 2017 IEEE Wireless Power Transfer Conference, 978-1-5090-4595-3/17
5. Parkin, K.L., DiDomenico, L.D., Culick, F.E.: The microwave thermal thruster concept. In: 2nd Intern. Symp. on Beamed Energy Propulsion, pp. 418–429, 0-7354-0175-6/04 (2004)
6. Hoff, B.W., Hilario, M.S., Jawdat, B., Baros, A.E., Dynys, F.W., Mackey, J.A., Yakovlev, V.V., Andraka, C.E., Armijo, K.M., Savrun, E., Rittersdort, I.M.: Millimeter wave interactions with high temperature materials and their applications to power beaming. In: Proc. 52nd IMPI Microwave Power Symp., Long Beach, CA, pp. 82–83, June 2018
7. Mohekar, A.A., Gaone, J.M., Tilley, B.S., Yakovlev, V.V.: A 2D coupled electromagnetic, thermal and fluid flow model: application to layered microwave heat exchangers. In: IEEE MTT-S Intern. Microwave Symp. Dig., Philadelphia, PA, pp. 1389–1392, June 2018
8. Mohekar, A.A., Gaone, J.M., Tilley, B.S., Yakovlev, V.V.: Multiphysics simulation of temperature profiles in a triple-layer model of a microwave heat exchanger. In: Proc. 52nd IMPI's Microwave Power Symp., Long Beach, CA, pp. 33–35, June 2018

9. Hilario, M.S., Hoff, B.W., Young, M.P., Lanagan, M.T.: W-band free-space dielectric material property measurement techniques for beamed energy applications. In: Proc. 53rd AIAA Aerospace Sciences Meeting, Kissimmee, FL, Jan 2015
10. Celuch, M., Kopyt, P.: Modeling of microwave heating of foods. In: Lorence, M.W., Pesheck, P.S. (eds.) Development of Packaging and Products for Use in Microwave Ovens, pp. 305–348. Woodhead Publishing, Cambridge (2009)
11. Yakovlev, V.V., Allan, S.M., Fall, M.L., Shulman, H.S.: Computational study of thermal runaway in microwave processing of Zirconia. In: Tao J. (ed.) Microwave and RF Power Applications, pp. 303–306 Cépaduès Éditions, Toulouse (2011)
12. QuickWave: QWED Sp. z o. o., http://www.qwed.eu/
13. Wang, S.J., Luechapattanaporn, K., Tang, J.: Experimental methods for evaluating heating uniformity in radio frequency systems. Biosyst. Eng. J. **100**, 58–65 (2008)